

34th CIRP Design Conference

Accelerated design of Power-to-X process chains for transient operation using Recurrent Neural Networks

Philipp Rentschler^{a,*}, Stefanie Baranowski, Christoph Klahn^{a,b}, Roland Dittmeyer^a

^aKarlsruhe Institute of Technology, Institute for Micro Process Engineering (IMVT), Hermann-von-Helmholtz-Platz 1, 76344 Eggenstein-Leopoldshafen, Germany

^bKarlsruhe Institute of Technology, Institute of Mechanical Process Engineering and Mechanics (MVM), Kaiserstraße 12, 76131 Karlsruhe, Germany

* Corresponding author. Tel.: +49-721-608-28451; fax: +49-721-608-23186. E-mail address: philipp.rentschler@kit.edu

Abstract

Climate change requires a reorientation towards renewable energy generation and storage technologies, especially from solar and wind-based sources. Power-to-X technologies offer a promising way to convert renewable energy into chemical energy carriers based on green hydrogen. A major obstacle to the implementation of such systems is the need to operate the plants dynamically to account for fluctuations. The conventional design of these process chains is usually done through complex dynamic flowsheet simulations, which require specialized engineers and are therefore time-consuming and costly.

This study presents an innovative approach to build surrogate models of process chains by using Recurrent Neural Networks and in detail Long Short-Term Memory. To establish a basis for the training data of these models, process simulations were performed with respect to critical parameters for plant dynamics and capacity adjustment. The developed models can represent the dynamics of the process and allow the estimation of annual production volumes for different geographical locations, based on local wind speeds. In addition, plant-specific variables, such as the number of cells in hydrogen-producing electrolysis, can be modified and optimized. These models open the possibility of making informed decisions at an early project stage and reduce the risk of implementing dynamic Power-to-X plants.

© 2024 The Authors. Published by Elsevier B.V.

This is an open access article under the CC BY-NC-ND license (<https://creativecommons.org/licenses/by-nc-nd/4.0>)

Peer-review under responsibility of the scientific committee of the 34th CIRP Design Conference

Keywords: Design methodology, tools and technologies; Design of X

1. Introduction and Motivation

Anthropogenic climate change represents one of the most pressing challenges of our time. It is alarming that despite growing awareness of the environmental impact of human activities, global greenhouse gas emissions as well as global primary energy demand continue to rise. Energy-intensive industries, particularly steel and chemicals, are major contributors to energy- and process-related greenhouse gas emissions at 8% and 5%, respectively [1].

Hydrogen is a promising energy source. Currently, it is mainly used in refineries and for ammonia synthesis. However, 95% of the hydrogen produced comes from fossil fuels, while only 0.7% is obtained from renewable sources [2]. With the

Climate Protection Act of June 21, 2023, Germany has set itself the goal of being greenhouse gas neutral by 2045 [3]. Hydrogen is seen as a key element in achieving the national climate targets. As part of the national hydrogen strategy, the German Federal Ministry of Education and Research is funding three flagship hydrogen projects. The H₂Mare project, for example, is investigating the production of green hydrogen and its downstream products directly at sea, using renewable energies from offshore wind farms and the electrolysis of water [4].

The production of chemical energy carriers from renewable electrical energy, referred to as Power-to-X (PtX), has the potential to transform sector coupling. However, PtX projects also follow the usual planning processes of chemical process engineering, which are divided into several phases, starting

with the rough conceptualization of different process configurations. This phase continues with the evaluation of efficiency and cost, followed by the detailed design of the plant components. During this development process, there is intensive interdisciplinary collaboration between engineers from different disciplines, with results from one area often directly influencing work in another [5]. However, process engineering projects, especially those involving dynamic process simulations in the context of fluctuating renewable energy, are characterized by considerable uncertainty. Such simulations are not only extremely resource intensive, but also require extensive expertise. In addition, local conditions, such as different wind speeds or solar irradiance, require individual considerations and adjustments of the PtX plant configurations. Therefore, there is an urgent need to transfer complex dynamic process simulations into fast and simplified surrogate models. Machine Learning (ML) models and in particular Recurrent Neural Networks (RNN) architectures are suitable for predicting non-linear time series behaviour and are used in various applications, such as manufacturing processes [6]. These models should be able to adequately represent the dynamics and at the same time make statements about plant dimensioning to efficiently derive production quantities and plant configurations during the development phase.

Considering this motivation and the challenges mentioned above, this work focuses on the development and validation of such surrogate models for hydrogen production. The goal is to provide a tool that is both accurate and resource efficient, thus making a valuable contribution to addressing the climate crisis.

To achieve this, a detailed flowsheet simulation is constructed to comprehensively characterize the dynamic behavior of the system. During the study, a RNN surrogate model is developed that aims to accurately reproduce the dynamic behavior of hydrogen production. Finally, the performance of the RNN surrogate model is critically evaluated and compared with the results of the flow sheet simulation.

2. Methods

The electrical energy required for hydrogen production through water electrolysis is obtained from renewable sources such as wind and solar. These energy sources naturally exhibit fluctuations that vary both on a large scale over years or seasons and on a small scale over daily cycles and in the range of seconds. These fluctuations lead to strong regional and temporal dependencies in PtX processes.

Process simulation is used in process engineering to predict production quantities and plant configurations. A distinction is made between steady-state and dynamic flowsheet simulation to design and evaluate dynamically operated plants that are exposed to natural fluctuations. The focus of this study is on the application of dynamic surrogate models of process simulations for the design of PtX process chains, especially in the context of wind turbines and proton exchange membrane (PEM) water electrolysis. It is analyzed how detailed process simulations can be transformed into simplified surrogate models without losing essential information about the dynamic behavior of the process chains required for design and

operation. These surrogate models are used by other engineering disciplines for the systems engineering.

In the first step, a detailed dynamic flowsheet simulation was created as ground truth to investigate the dynamic behavior and to generate data sets for training, validation and testing. RNN models were then created as the surrogate models and compared with the flowsheet simulations. The methods described in detail below were applied to evaluate the suitability of these approaches for modeling PtX process chains.

2.1. Dynamic flowsheet simulation as reference model

The tool "AVEVA Process Simulation" (APS) was used to model and simulate complex process plants. It allows a holistic representation of process chains and the integration of physically and chemically based equation systems. The model structure is divided into three consecutive phases: Process Mode for steady-state calculations where flow is determined by flow rates. Fluid Mode, where the flow is based on a given pressure, which is particularly useful for designing piping systems. Transient energy and mass balance equations are considered at this stage. Dynamic Mode for time-dependent calculations using defined time steps and considering unsteady energy and mass balance equations.

2.1.1. Wind turbine simulation

A standard model from the APS library was used to characterize the wind park. A wind turbine converts the kinetic energy of the wind into electrical energy, where the mechanical power of the turbine is calculated according to the formula (1).

$$P_w = \frac{1}{2} \cdot \rho \cdot A \cdot v_w^3 \cdot C_p \quad (1)$$

The characterization of wind turbines is carried out by means of power curves representing the mechanical power as a function of wind speed v_w . The formula also includes the rotor area A , the power coefficient C_p and the air density ρ . The characterization parameters such as nominal power P_{rated} , cut-in and cut-out wind speed are determined from these curves.

The underlying wind data include wind speed measurements at 12 wind turbines distributed over a rectangular area with dimensions 4x4 km² [7]. This wind data has a resolution of one second and cover a period of 30 consecutive days. Based on this data set, wind data sets with varying sampling rates can be generated for all 12 wind turbines. The names and properties of the data sets used for the simulations are listed in Table 1.

2.1.2. Electrolysis model

A PEM electrolysis model simulates the transient hydrogen production (Fig. 1). The molar hydrogen flow produced in a stack $\dot{n}_{H_2,stack}$ is proportional to the number N_{cell} and the electric current I_{cell} of a cell and is calculated according to formula 2 with the Faraday efficiency η_f , the Faraday constant

Table 1. Overview of the generated wind data sets

Dataset	T1_1sec	T1_1min	T1_5min	T1_15min	T5_5min
Resolution	1	60	300	900	300
T_s in s					
Number of data points	2592000	43200	8640	2880	8640
Turbine Number	1	1	1	1	5

Table 2. Characteristics of the modeled PEM electrolyzer

PEM Electrolyzer	
Number of stacks ($N_{parallel}$)	4
Number of cells (N_{cell})	40
Rated power in kW (P)	100
Load range in %	5 - 104
H ₂ - production at nominal load in kg/h	2.1
Stack current in A	353
Stack voltage in V	57.3 - 68.4
Temperature range in °C	55.5 - 67.5
System pressure in bar	48

F and the charge number z . Polarization curves characterize electrolytic cells, where cell voltage U_{cell} is plotted versus current density i_{dense} , with constant electric power of the electrolyzer [8].

$$\dot{n}_{H_2,stack} = N_{cell} \cdot \eta_f \cdot \frac{I_{cell}}{z \cdot F} \quad (2)$$

In the context of renewable energy systems, electrolysis plants need to cope with wind fluctuations and to minimize buffer capacities, flexible and adaptive plant operation is required. In this regard, PEM electrolysis represents a particularly suitable technology to follow fluctuating electric power due to its short cold and hot start-up times and high load gradients of 10% nominal power change per second [9].

2.1.3. Coupling of the wind turbines with the PEM electrolyzer model

The direct coupling between the wind turbine and the PEM electrolyzer was investigated in a dynamic process simulation to analyze the effects of wind speed fluctuations on electricity production and thus on hydrogen production.

An overarching goal was to map a hot standby state of the electrolyzer as a function of electrical power and wind speed. Hot standby represents a state of readiness in which the system is maintained at operating pressure and temperature without producing hydrogen e.g. in times of energy shortage. The PEM electrolyzer can be operated at cell level up to 0% partial load, but the energy self-consumption of the peripheral components sets the lower power limit to about 5% of the nominal power [10]. This required power for the hot standby could be provided by a battery. The correlation between wind speed and wind turbine power depends on the underlying power curve.

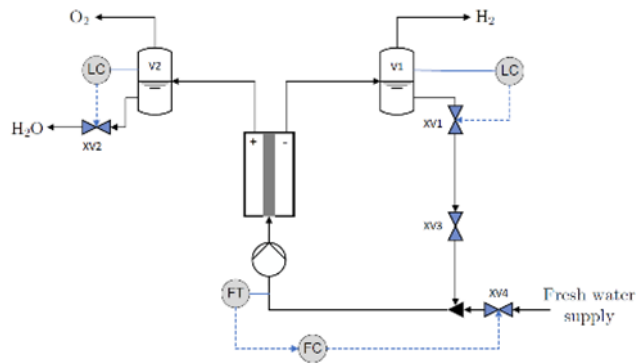


Fig. 1. Schematic structure of the PEM electrolyzer.

In the given simulation setup, the 5% power is achieved at a wind speed of $v_w = 4.83 \text{ m/s}$. In order to be able to represent the hot standby in the training data, the minimum wind speed in the wind data set used was thus set to this windspeed and the corresponding hydrogen production to 0 kmol/s.

2.2. Surrogate modeling using Machine Learning

Machine learning (ML) represents an approach in which software is trained based on existing data to learn a function f that represents the relationship between input variables X (features) and output variables Y (labels). In regression, where the target variables Y represent continuous values, the relationship f is to be learned. The available set of examples, based on which the function f is learned, is called training data. The ML models can now receive new values for X and make a prediction for Y based on the learned function f . In the presence of the target variable Y in the training data set, this is called supervised learning.

To build and evaluate ML models, three data sets are needed: Training data, test data, and validation data. The training data is used to learn the relationship between features and target variables, while the validation and test data, which are not used in training, are used to fit the hyperparameters and check the generalizability of the model, respectively. Adjustment of the hyperparameters, which are related either to the structure of the model or to the settings of the learning algorithm, is performed using the validation data until the $X \rightarrow Y$ mapping is optimized. A loss function, e.g., mean square error (MSE), can be used to quantify the deviation between the actual value and the predicted value.

2.2.1. Recurrent Neural Networks (RNN) and Long-Short-Term-Memory (LSTM)

Artificial neural networks (ANN) are ML models inspired by biological neural networks. An artificial neuron is modeled after the operation of a biological neuron by summing input signals over weighted connections, adding a bias, and applying an activation function. This type of artificial neuron is also called a Linear Threshold Unit because of the linear activation function.

A multi-layer perceptron (MLP) is a specific form of ANN that consists of multiple layers of neurons. It has one or more hidden layers of neurons, and the last layer is called the output layer. A weight connects the neuron of the current layer to the

neuron of the previous layer. To train a neural network means to adjust the weights. An activation function is applied to each neuron and the output is passed to the next layer. Unlike MLPs, where activation of neurons occurs in only one direction, RNN and LSTM networks allow connections in other directions [6].

Feature selection is critical to modeling. Relevant model parameters are necessary to adequately represent the behavior of the system being modeled, while irrelevant or redundant features do not improve the predictive power of the model and only generate noise without improving the performance of the model [11].

2.2.2. Model configuration of the LSTM-RNN

The open-source framework TensorFlow in combination with Keras was used to develop the ML surrogate models, with modeling performed using LSTM-RNN. The wind speed v_w and the number of parallel stacks $N_{parallel}$ served as features, while the hydrogen flow \dot{n}_{H_2} was defined as label Y . Here, $N_{parallel}$ represents the number of parallel stacks, which serves as a variable for capacity adjustment of the electrolyzer.

A scale-up of the overall system was performed in the flow sheet simulator with the goal of being able to represent higher capacity ranges in the training data. The scaling involved the following parameters, which were increased at the same rate as the rated power of the electrolyzer: The number of wind turbines in the wind farm, the fresh water flow rate, the number of stacks in the electrolyzer, the volume of the separation tank, and the flow coefficient c_v of the valve in the recycle stream.

A total of five simulations were set up in the flowsheet simulator, whose names and characteristics are listed in Table 3. Except for the PEM_700 simulation, all simulations are based on the T1_5min wind data set, whereas the T5_5min data set was used for PEM_700. The determined hydrogen flow was recorded in intervals of 300 seconds.

The neural network was trained to predict the hydrogen flow \dot{n}_{H_2} using sequential wind data and the number of stacks as input variables. The data set PEM_200 served as validation data set, while PEM_700 was selected as test data set due to a different wind trend. In each case, the entire wind dataset for the entire month was used. The LSTM-RNN was trained using the PEM_100, PEM_400 and PEM_1000 datasets. The network architecture consisted of an LSTM-RNN trained using the sliding window method. A window size of $l_{window} = 10$ was specified. Labels Y and features X were separated before processing the training data. Since most ML models, including neural networks, learn more inefficiently when the input sizes vary, the features were normalized. The batch size refers to the number of X_{train} and Y_{train} pairs processed by the algorithm before the weights are updated. An epoch refers to the number of iterations over all training data, after which all training data pairs X_{train} and Y_{train} were used once for training. The LSTM-RNN was composed of three hidden layers consisting exclusively of LSTM neurons. No activation function was applied to the LSTM neurons. The output layer was a dense layer with one neuron, and the “ReLU” activation function was used for the output neuron. To avoid overfitting, the regularization method Dropout with a dropout rate of 40% was applied between the 2nd and 3rd hidden layers (Table 4). Additionally, the Keras module “ModelCheckpoint” was used

to monitor the validation loss and store the model with the lowest validation loss. This model was then used for the predictions.

Table 3. Simulation setup and the wind data used for the scale-up.

Dataset	PEM_100	PEM_200	PEM_400	PEM_700	PEM_1000
Rated power electrolyzer in kW	100	200	400	700	1000
Number of wind turbines	1	2	4	7	10
Number of stacks	4	8	16	28	40
Separator volume in m ³	1	2.1	4.2	7.3	10.5
Separator height, length in m	1	1.3	1.6	1.9	2.2
Wind dataset	T1_5min	T1_5min	T1_5min	T5_5min	T1_5min

Table 4. Structure and hyperparameters of the RNN.

Hyperparameter	Value
1. Hidden layer	32 LSTM neurons
2. Hidden layer	16 LSTM neurons
Dropout layer	40% Dropout rate
3. Hidden layer	4 LSTM neurons
Output layer	Dense layer with one neuron
Activation function	ReLU
Learning rate η	0.0001
Loss function	MSE
Batch size	60
Training epochs	300

3. Discussion of the results

In the following section, the results of the flowsheet simulations and the RNN surrogate models based on them are presented and discussed.

3.1. Flowsheet simulation of PEM electrolyzer and influence of wind data resolution

The studied electrolyzer model was simulated with a maximum power of 104% of the nominal power after conduction and conversion losses, with a minimum load limit of 5% of the nominal load due to the hot standby assumption (Fig. 2). At a temperature of 60°C, the current density i_{dens} equals 1.22 A/cm² and the cell voltage U_{cell} equals 1.76 V. The values are within the range of experimentally determined polarization curves [12].

The effects of data resolution on the accuracy of the hydrogen production rate in APS were investigated by comparing the simulation results of the same underlying wind data set at 1 second, 1 minute, 5 minutes, and 15 minutes resolutions (Fig. 3). The coefficient of determination for $T_s = 1$ min is $R^2 \approx 0.992$. For $T_s = 5$ min and $T_s = 15$ min, the coefficient of determination is $R^2 \approx 0.934$ and $R^2 \approx 0.757$,

respectively. As expected, it is found that finer resolution of the wind data improves the quality of the flowsheet simulation.

For $T_s = 1 \text{ min}$ or a sampling rate of 16.7 mHz , it results accordingly that a maximum of frequency components of 8.35 mHz can appear in the wind data. The deterioration of the results at a larger T_s -value indicates that the high frequency components from 8.35 mHz to a maximum of 0.5 Hz are not completely filtered out by the system and are therefore visible in the hydrogen stream.

3.2. RNN surrogate modeling

The coefficient of determination R^2 for the prediction of the test data is 0.94 . The test data vary in the range of $\dot{n}_{H_2} = 0 \text{ kmol/s}$ to $2 \cdot 10^{-3} \text{ kmol/s}$. The predicted hydrogen flow ranges up to $2.4 \cdot 10^{-3} \text{ kmol/s}$. The hydrogen n_{H_2} produced in the whole month is determined. According to the flowsheet simulation, the value is $n_{H_2,FS} = 885.16 \text{ kmol}$, while the RNN predicts a total production of $n_{H_2,RNN} = 956.65 \text{ kmol}$. This represents a relative deviation of 8% with respect to $n_{H_2,FS}$.

The largest absolute deviation between the test data and the prediction is $\dot{n}_{H_2} = 8.7 \cdot 10^{-4} \text{ kmol/s}$ at time $t = 1.5258 \cdot 10^6 \text{ s}$ (Fig. 4 (a)). The time period shown includes the prediction with the largest absolute deviation. Fig. 4 (b) shows the hydrogen flow in kmol/s versus time. The shown period corresponds to a 24-hour period from day 27 to 28. Calculating the coefficient of determination exclusively for the values in this 24-hour period yields a value of $R^2 \approx 0.92$.

In the range from $2.35 \cdot 10^6 \text{ s}$ to $2.36 \cdot 10^6 \text{ s}$ and $2.378 \cdot 10^6 \text{ s}$ to $2.388 \cdot 10^6 \text{ s}$, it can be seen that the neural network overestimates the hydrogen flow. The hydrogen flow briefly drops to zero, but the prediction does not follow this downward outlier. From second $2.393 \cdot 10^6 \text{ s}$, a wind lull sets in and no hydrogen is produced until $2.412 \cdot 10^6 \text{ s}$. The neural network prediction is 0 kmol/s . The short outlier during the wind lull is also predicted but underestimated in magnitude.

The possibility of scaling up the electrolysis capacity was successfully implemented in the RNN model. However, the validity of the RNN surrogate model is limited by the training data used. The training data varied from 4 to 40 stacks, or a capacity of 100 kW to 1 MW respectively, and the Balance of plant (BoP) had to be maintained or scaled up accordingly. The RNN was able to reproduce the hot standby condition. PEM electrolyzers can ramp up from hot standby to full load operation in less than 10 seconds [9].

Since there are 300 seconds between two time steps, abrupt changes in hydrogen production, as shown in Fig. 4 (b), are physically possible. The discrepancy in the prediction of the sudden wind drop can be explained by the training structure of the RNN: it is based on the current and the last 9 ($l_{window} = 10$) wind data. The drop in production occurs abruptly and is not evident from the trend of the previous values. Presumably, this situation was not sufficiently represented in the training data and it would be necessary to retrain with greater variability in the wind data, especially for sudden wind drops.

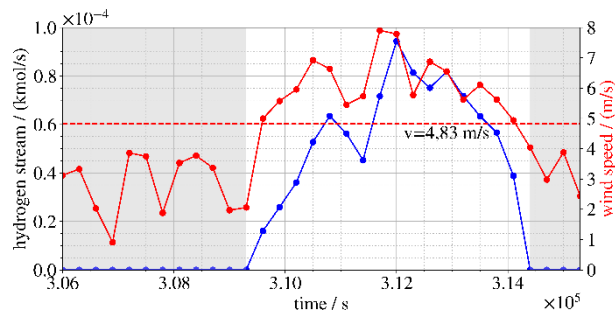


Fig. 2. Wind speed and hydrogen production over time. The hot standby is simulated in the gray shaded areas.

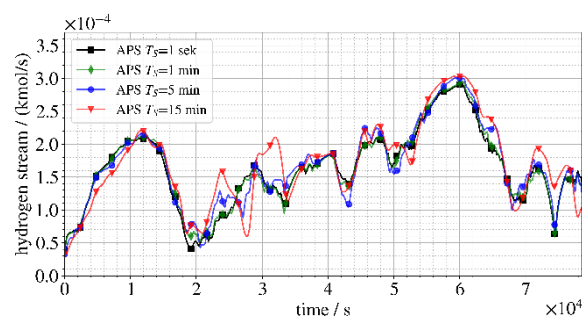


Fig. 3. Hydrogen flow calculated by flowsheet simulation at different wind resolutions as a function of time.

For the test data set, wind data and an electrolyzer setup were used that were not previously part of the training. Therefore, the test data is well suited to evaluate the generalizability of the RNN model. The neural network overestimates the hydrogen flow for the test data by 8% , and the coefficient of determination is $R^2 \approx 0.94$. Thus, an RNN model was developed that can replace the flowsheet simulation with sufficient accuracy.

3.3. Integration into the PtX design process

The integration of RNN models into the PtX design process not only accelerates iteration loops and supports more efficient decision making in early stages of development, but also enables faster investment appraisal and bottleneck identification. The use of RNN-based model information, which does not require a detailed understanding of the complex underlying models, facilitates interdisciplinary collaboration, and extends it to other areas such as models for life cycle and techno-economic analysis.

The reduction of complexity throughout the design process promotes the use of optimization tools and increases the ability to efficiently evaluate and compare design alternatives. In particular, the use of RNN enables the simulation and evaluation of different operating conditions, which is crucial for the design and optimisation of PtX systems. The effective integration of dynamic input data, such as wind speed, into site evaluation and capacity planning leads to a fast and adaptive optimisation of PtX processes. The extension of the operating ranges analysed allows for accelerated plant scale-up in the design process, as larger system capacities can be mapped. The possibility of increasing the accuracy of the models through the future use of transformer models opens further prospects.

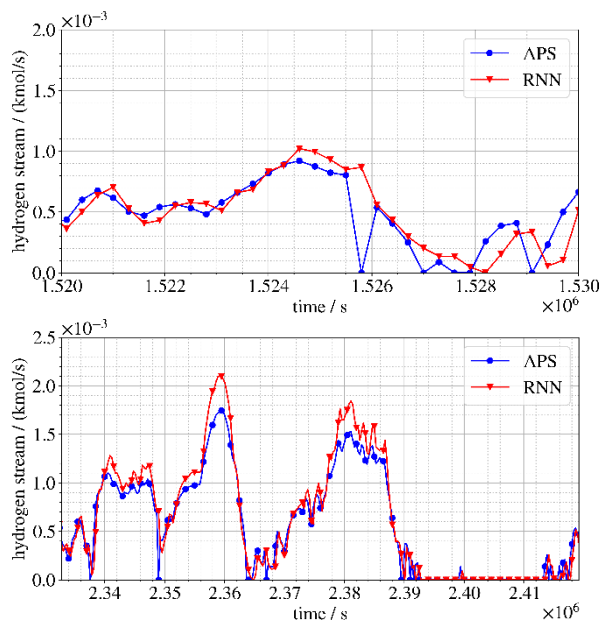


Fig. 4. (a) Comparison between the calculated hydrogen flow by the flowsheet simulation and the prediction of the RNN; (b) with simulated hot standby during a wind lull.

4. Conclusion

In this study, two methods for evaluating the transient behavior of Power-to-X process chains were discussed: conventional process simulations and machine learning-based surrogate models. Dynamic process simulations are used for detailed design and sizing of individual components but require extensive expert knowledge and are time-consuming.

On the other hand, there are the dynamic surrogate models, which are based on process simulations but can effectively and more resource-efficiently represent the dynamic behavior in the system development process. Initially, a PEM electrolysis system was designed in the flow sheet simulator AVEVA Process Simulation. The influence of wind resolution on the dynamics of hydrogen production was investigated. As expected, the quality of the flowsheet simulation improves with finer resolution of the wind data. In a further step, a LSTM-RNN surrogate model was developed to dynamically predict the hydrogen flow. The created model uses only the wind speed and the number of stacks for prediction. A scale-up is performed to be able to represent electrolysis systems between 100 kW and 1 MW nominal power with this model.

In conclusion, the LSTM-RNN surrogate models can be used with good accuracy to draw quick conclusions about hydrogen production rates under various fluctuating wind data and are a powerful tool in the design process by accelerating, simplifying and increasing adaptability. Their ability to be quickly integrated into various applications makes them ideal for use in other specialist areas, such as the simulation of energy systems or in digital twins and accelerate the process chain design of different sites and applications in the future.

Acknowledgements

This contribution was funded by the Federal Ministry of Education and Research (BMBF) under grant 03HY302A.

Declaration of generative AI in the writing process

During the preparation of this work the author used ChatGPT and DeepL in order to improve readability. After using these tools, the author reviewed and edited the content as needed and takes full responsibility for the content of the publication.

References

- [1] International Renewable Energy Agency (IRENA), *Green hydrogen for industry: A guide to policy making*, 2022.
- [2] International Renewable Energy Agency (IRENA), *Hydrogen: a renewable energy perspective*. Abu Dhabi: International Renewable Energy Agency, 2019.
- [3] Press and Information Office of the Federal Government, “Ein Plan fürs Klima: Klimaschutzgesetz und Klimaschutzprogramm.” [Online]. Available: <https://www.bundesregierung.de/breg-de/aktuelles/klimaschutzgesetz-2197410>
- [4] Federal Ministry of Education and Research, “How partners in the H2Mare flagship project intend to produce hydrogen on the high seas.” [Online]. Available: <https://www.wasserstoff-leitprojekte.de/projects/h2mare>
- [5] M. Kleiber, *Process engineering: addressing the gap between studies and chemical industry*. in De Gruyter textbook. Berlin ; Boston: Walter de Gruyter GmbH & Co, 2016.
- [6] B. Lindemann, T. Müller, H. Vietz, N. Jazdi, and M. Weyrich, “A survey on long short-term memory networks for time series prediction,” *Procedia CIRP*, vol. 99, pp. 650–655, 2021, doi: 10.1016/j.procir.2021.03.088.
- [7] M. Anvari et al., “Short term fluctuations of wind and solar power systems,” *New J. Phys.*, vol. 18, no. 6, p. 063027, Jun. 2016, doi: 10.1088/1367-2630/18/6/063027.
- [8] A. Buttler and H. Spliethoff, “Current status of water electrolysis for energy storage, grid balancing and sector coupling via power-to-gas and power-to-liquids: A review,” *Renewable and Sustainable Energy Reviews*, vol. 82, pp. 2440–2454, Feb. 2018, doi: 10.1016/j.rser.2017.09.003.
- [9] H. Lange, A. Klose, W. Lippmann, and L. Urbas, “Technical evaluation of the flexibility of water electrolysis systems to increase energy flexibility: A review,” *International Journal of Hydrogen Energy*, vol. 48, no. 42, pp. 15771–15783, May 2023, doi: 10.1016/j.ijhydene.2023.01.044.
- [10] J. Töpler and J. Lehmann, Eds., *Hydrogen and Fuel Cell: Technologies and Market Perspectives*. Berlin, Heidelberg: Springer Berlin Heidelberg, 2016. doi: 10.1007/978-3-662-44972-1.
- [11] R. May, G. Dandy, and H. Maier, “Review of Input Variable Selection Methods for Artificial Neural Networks,” in *Artificial Neural Networks - Methodological Advances and Biomedical Applications*, K. Suzuki, Ed., InTech, 2011. doi: 10.5772/16004.
- [12] M. Espinosa-López et al., “Modelling and experimental validation of a 46 kW PEM high pressure water electrolyzer,” *Renewable Energy*, vol. 119, pp. 160–173, Apr. 2018, doi: 10.1016/j.renene.2017.11.081.